Phonon dispersion on a GaAs(110) surface studied using the adiabatic bond charge model

1996 J. Phys.: Condens. Matter 8 1345

(http://iopscience.iop.org/0953-8984/8/10/007)

J. Phys.: Condens. Matter **8** (1996) 1345–1358. Printed in the UK

Phonon dispersion on a GaAs(110) surface studied using the adiabatic bond charge model

H M Tütüncü and G P Srivastava
Department of Physics, Exeter University, Exeter EX4 4QL, UK

Received 24 July 1995, in final form 15 November 1995

Abstract. We have used the adiabatic bond charge model within a repeated slab scheme to study lattice dynamics on the GaAs(110) surface. The results provide a more detailed analysis of the surface phonon modes than is available from existing theoretical and experimental techniques.

1. Introduction

The clean cleaved III–V(110) surfaces have in general been the subject of intensive research over the past thirty years. While most experimental and theoretical studies have been devoted to determination of surface atomic geometry and surface electronic states, only in the recent past have surface vibrational properties been investigated. The GaAs(110) surface is the most commonly studied, and therefore the prototypical cleaved semiconductor surface. Low-energy electron diffraction analysis [1] and medium-energy ion-scattering experiments [2] have determined the relaxed atomic geometry of GaAs(110). Angle-resolved photoemission studies [3] have mapped out occupied surface electronic states along symmetry directions on the surface Brillouin zone. Total energy pseudopotential calculations [4–6] have confirmed the experimental results for the equilibrium geometry and for the occupied surface electronic states. Recently, quasi-particle calculations have been made [7, 8], which indicate that the band gap of GaAs is free from any surface electronic states, in agreement with the conclusion reached from a combination of direct and inverse photoemission measurements [9]. Low-energy (i.e. acoustic) surface phonon modes on GaAs(110) were detected with inelastic He-atom-scattering experiments [10]. High-resolution electron energy-loss spectroscopy (HREELS) has been used to study both low-energy and high-energy surface phonon modes [11–18].

The experimental studies, using inelastic He-atom scattering and HREELS as mentioned above, do not provide an unambiguously clear picture of atomic vibrations on the GaAs(110) surface. Both techniques are unable to detect atomic displacements which are strictly horizontal (such as the so-called A″ modes along $\overline{\Gamma}$–$\overline{X}'$—see later). Moreover, while higher energies are not accessible for He-atom scattering, different HREELS studies have placed surface vibrational energies at somewhat different positions. In particular, the number of surface acoustic modes and their energy positions are reported to be different by different groups.

On the theoretical side, the phenomenological bond charge model (BCM) [19, 20], a tight-binding model [21–23], and *ab initio* pseudopotential schemes [24–26] have been used to study surface vibrations on GaAs(110). However, there is a lack of detailed understanding

0953-8984/96/101345+14$19.50

of various surface modes and their characters (i.e. polarization and localization). In particular, *ab initio* calculations are computationally very demanding and have thus mainly been made for a selected number of high-symmetry points in the surface Brillouin zone [24–26]. Only one group [25] has presented *ab initio* results for surface phonon dispersion along the azimuths $\overline{\Gamma}$–$\overline{X}$ and $\overline{\Gamma}$–$\overline{X}'$ (see figure 1). In their work Fritsch *et al* [25] used a linear response approach, based on the density functional perturbative scheme, to achieve this. Santini *et al* [19, 20] have studied surface phonon dispersion curves on GaAs(110) and Ge(111) 2×1 using the adiabatic BCM. They used six adjustable force-constant parameters and expressed an appropriate new equilibrium condition for the GaAs(110) surface, and obtained phonon frequencies in reasonably good agreement with data on He inelastic scattering up to 15 meV energy. However, a wealth of HREELS data have recently become available [17, 18] along three symmetry directions up to phonon energies of 40 meV. It is thus interesting to calculate surface phonon dispersion and mode polarization characteristics along various symmetry directions over the entire frequency range using a single theoretical approach such as the BCM. A comparison of the BCM results with those obtained from *ab initio* calculations and HREELS measurements would establish the BCM as a reliable theoretical tool for such studies.

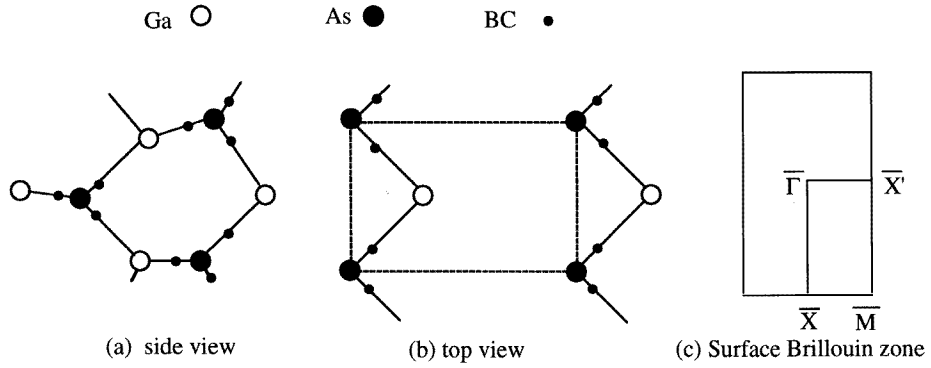

Figure 1. Schematic (a) side and (b) top views of the relaxed surface geometry of the GaAs(110) surface. The surface Brillouin zone is shown as (c).

In this paper we present a detailed account of phonon frequencies and polarization of atomic vibration along various symmetry directions in the Brillouin zone for the GaAs(110) surface by applying the adiabatic BCM to the recently determined relaxed atomic geometry [6]. In particular, we discuss the effect of surface relaxation on surface phonon frequencies, and compare our findings with the up-to-date experimental and *ab initio* theoretical investigations. We find that while the displacement patterns remain largely unchanged, some surface frequencies shift upwards by up to 3 meV when the relaxation of ionic and bond charge (BC) positions is considered in our calculation. Our results for the relaxed surface geometry are in very good overall agreement with experimental data and the *ab initio* work of Fritsch *et al* [25] over the entire frequency range. We also agree with Santini *et al* that the ion–BC force-constant matrix plays an important role in the study of surface dynamics, while the surface ion–ion force-constant matrix is nearly the same as the bulk force-constant matrix.

2. Theory

The phenomenological adiabatic BCM was originally devised by Weber to study the lattice dynamics of tetrahedrally coordinated semiconductors [27–29]. This model produces bulk phonon dispersion curves which are in good agreement with experimental neutron scattering data, for both homopolar and heteropolar semiconductors. Also, in a previous study it was found [30] that this model predicts dispersions of eigenvalues and eigenvectors of lattice vibrations in bulk semiconductors which are in good agreement with *ab initio* calculations. The number of adjustable parameters is four for homopolar semiconductors (such as Si) and six for heteropolar semiconductors (such as GaAs). The method has been successfully applied in studying vibrational modes of semiconductor surfaces [19, 20, 31] and fullerenes [32].

In the BCM for tetrahedrally bonded semiconductors, the valence electron charge density distribution is represented by massless bond charges (BCs), endowed with translational degrees of freedom. The BCs are displaced towards anions, dividing a bond in the ratio 3:5 in A^3B^5-type semiconductors. The BCs are allowed to move adiabatically, following the ionic displacements so as to keep in equilibrium with the instantaneous positions of the ions. In this paper, we have used the results of a recent *ab initio* pseudopotential calculation for the atomic geometry of the GaAs(110) surface [6]. As seen from figure 1, the top-layer Ga atoms move towards the bulk while the top-layer As atoms move away from the bulk. The positions of the dangling BCs are decided according to the maximum valence electron density [6]. We consider an artificially periodic slab geometry, as used in total energy and band-structure calculations [6]. In the present case a supercell is considered to contain eleven (110) layers of GaAs and a vacuum region equivalent to nine layers of GaAs. In the plane normal to [110] the unit cell is considered to have a 1×1 structure. Thus a relaxed unit cell contains 22 ions and 44 BCs. Our choice of the slab size is somewhat better than that considered in recent *ab initio* works [24–26] and is adequate for examining atomic vibrations of up to top three surface layers. It is appropriate at this point to mention that in their calculations Santini *et al* modelled the surface as a semi-infinite crystal in the form of a slab of 23 layers rather than in the form of a repeated slab as considered in this work.

We have examined the dependence of mode frequencies on the thickness of the vacuum layer in the unit cell. We find that the lowest surface frequency at the $\overline{\mathrm{M}}$ point in the surface Brillouin zone (see figures 1 and 2) turns out to be 6.74, 7.15, 7.11, 7.12, 7.12 and 7.12 meV when the vacuum region is taken to be equivalent to 1, 2, 4, 6, 9 and 11 atomic layers, respectively. We thus find that our choice of nine layers for the vacuum region is totally adequate.

For the application of the BCM we have considered three types of interaction.

(i) In order to calculate long-range Coulomb interactions, we assume that the two ionic charges are equal, $Z_1 = Z_2 = -2Z$, where Z is the bond charge. The Coulomb matrix is of size 198×198, corresponding to a total of 66 charged particles in the relaxed unit cell:

$$C^C_{\alpha\beta=x,y,z}(\kappa\kappa'|\boldsymbol{q}) = \frac{e^2}{V_a}\frac{Z^2}{\varepsilon}\begin{bmatrix} 4C_R & -2C_T \\ -2C_T^+ & C_S \end{bmatrix}$$

where C_R, C_T, C_T^+, C_S denote the ion–ion, ion–BC, BC–ion and BC–BC matrices, respectively. ε is the dielectric constant and V_a is the volume of the unit cell (20 times the bulk unit-cell volume). Z^2/ε is known as the force-constant parameter for Coulomb interaction and is taken as its bulk value [29]. These matrices are calculated by a Ewald technique [33]. Using the translational symmetry of the Coulomb force constants [33],

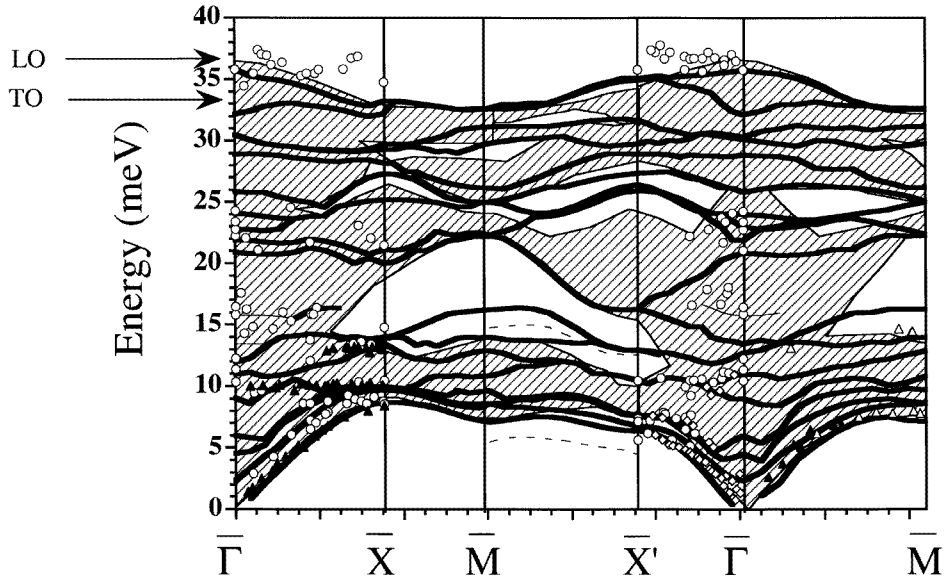

Figure 2. The dispersion of surface phonon modes on the GaAs(110) surface. The calculated results for the relaxed surface geometry are shown by thick solid curves. The results for the ideally terminated surface geometry are shown by dashed curves. Modes with complex displacement patterns with large amplitude at the outermost surface atoms are shown by thin curves. Also shown are experimental results taken from: (a) He-atom-scattering data (open and closed triangles [10, 20], and open diamonds [16]); (b) HREELS data (open circles [17, 18]).

it can be shown that the self-term ion–ion Coulomb force-constant matrices are non-zero because of broken bulk symmetry in the presence of the surface. In addition, we find that in the surface region the ion–ion and BC–BC self-term matrices are very sensitive to atomic geometry.

(ii) Let ϕ_1 and ϕ_2 denote the two ion–BC central potentials and ϕ_{i-i} show the nearest-neighbour interaction potential of ions. BCs also interact directly with each other via potentials ψ_1 and ψ_2, depending on whether they are centred around ion 1 or ion 2. Following Rustagi and Weber [29] we assume $\psi_1' = \psi_2' = 0$. In order to get the first derivative of ϕ_1, ϕ_2, and ϕ_{i-i}, we have imposed the equilibrium condition for the unit cell described above. The second derivatives of potentials do not appear for this equilibrium condition and thus we take them as their bulk values. This choice is also in agreement with the observation [1, 5, 6] that at and near the surface the relative ion–BC, ion–ion and BC–BC distances are nearly the same as the bulk values (the so-called bond-conserved surface relaxation model). The central-force-constant matrix connecting two particles can be calculated as [33]

$$\Phi_{\alpha\beta}(\ell\kappa;\ell'\kappa') = \frac{x_\alpha x_\beta}{r^2}\left[\phi''_{\kappa\kappa'}(r) - \frac{1}{r}\phi'_{\kappa\kappa'}(r)\right] + \frac{\delta_{\alpha\beta}}{r}\phi'_{\kappa\kappa'}(r) \tag{1}$$

where r denotes magnitude of the relative distance between particle κ in the ℓth unit cell, and κ' in the ℓ'th unit cell, and $\phi_{\kappa\kappa'}$ represents inter-particle central potential (i.e. ϕ_1, ϕ_2, ϕ_{i-i}, ψ_1 or ψ_2 as the case may be). As seen from this equation, the central-force-constant matrix connecting two particles also depends on the components of the relative distance between particles (i.e. x_α, x_β). For this reason, the central-force-constant matrices connecting top-

layer atoms and BCs are very different from the bulk values, indicating clearly that a careful consideration of the ion–BC force-constant matrix is very important for a study of surface dynamics.

(iii) We have taken bond-bending forces into account by using the Keating bond-bending potential [34]. Any two BCs i, j, centred around a common ion σ, interact with each other and with the ion via a Keating potential

$$V_{bb}^{(\sigma)} = \frac{1}{2} B_\sigma (\boldsymbol{X}_{\sigma i} \cdot \boldsymbol{X}_{\sigma j} + a_\sigma^2)/4a_\sigma^2 \tag{2}$$

where $\boldsymbol{X}_{\sigma i}$, $\boldsymbol{X}_{\sigma j}$ are the distance vectors connecting ions σ ($\sigma = 1, 2$) to BCs i, j, B_σ are force constants, and a_σ^2 is the equilibrium value of $|\boldsymbol{X}_{\sigma i}.\boldsymbol{X}_{\sigma j}|$. Since this potential depends only on scalar products, the rotational invariance condition is fulfilled. The elements of the short-range Keating ion–BC matrices connecting a top-layer As atom and its neighbouring BCs become very much bigger than the corresponding bulk values because the angles between neighbouring BCs change considerably on the relaxed surface. This is the second reason for which a proper consideration of the surface ion–BC interaction is very important. In addition, the Keating force-constant matrices connecting top-layer Ga atoms and BCs are also different from bulk values because on the relaxed surface Ga atoms are surrounded by three BCs instead of four.

Short-range force-constant matrices are divided into the ion–ion force-constant matrix R, the ion–BC force-constant matrix T, and the BC–BC force-constant matrix S. In the matrix notation, the dynamical equations for the ions and BCs are

$$M\omega^2 \boldsymbol{U} = \left[R + \frac{4Z^2}{\varepsilon} C_R\right] \boldsymbol{U} + \left[T - \frac{2Z^2}{\varepsilon} C_T\right] \boldsymbol{W} \tag{3}$$

$$m\omega^2 \boldsymbol{W} = \left[T^+ - \frac{2Z^2}{\varepsilon} C_T^+\right] \boldsymbol{U} + \left[S + \frac{Z^2}{\varepsilon} C_S\right] \boldsymbol{W} \tag{4}$$

where M and m are the ion and BC mass matrices respectively, and $\boldsymbol{U}$ and $\boldsymbol{W}$ are column matrices in $\boldsymbol{q}$-space (wave-vector space) denoting, respectively, the displacements of ions and BCs in the unit cell. In the adiabatic approximation ($m = 0$), we have

$$\boldsymbol{W} = -\left[S + \frac{Z^2}{\varepsilon} C_S\right]^{-1} \left[T^+ - \frac{2Z^2}{\varepsilon} C_T^+\right] \boldsymbol{U}. \tag{5}$$

With this we get

$$M\omega^2 \boldsymbol{U} = C^{total} \boldsymbol{U} \tag{6}$$

where C^{total} is the effective ion–ion C-type matrix, which can be written as

$$C^{total} = \left[R + \frac{4Z^2}{\varepsilon} C_R\right] - \left[T - \frac{2Z^2}{\varepsilon} C_T\right] \left[S + \frac{Z^2}{\varepsilon} C_S\right]^{-1} \left[T^+ - \frac{2Z^2}{\varepsilon} C_T^+\right]. \tag{7}$$

Note that C^{total} is a square matrix of order $3n$ where n is the number of atoms in the unit cell. The branches of the dispersion relations $\omega_j^2(\boldsymbol{q})$ with $j = 1, 2, \ldots, 3n$ are the solutions of the secular equation

$$\left[\frac{1}{M} C^{total}(\boldsymbol{q}) - \omega^2 I\right] \boldsymbol{U}(\boldsymbol{q}) = 0. \tag{8}$$

Atomic displacements can be expressed in terms of the eigenvectors of the dynamical eigenvalue problem. For the C-type dynamical matrix, the actual displacement of the atom $\ell\kappa$ in the mode $\boldsymbol{q}j$ is given by [33]

$$\boldsymbol{u}(\ell\kappa|\boldsymbol{q}j) = \frac{1}{\sqrt{M_\kappa}} \boldsymbol{U}(\kappa|\boldsymbol{q}j) \exp\{\mathrm{i}\,[\boldsymbol{q} \cdot \boldsymbol{x}(\ell\kappa) - \omega t]\} \tag{9}$$

where $\boldsymbol{x}(\ell\kappa) \equiv \boldsymbol{x}(\ell) + \boldsymbol{x}(\kappa)$ is the equilibrium position vector of the κth atom with mass M_κ in the ℓth unit cell.

3. Results

In figure 2 we have plotted the projected bulk GaAs phonon energies (hatched regions) and surface phonon energies along various symmetry directions in the irreducible part of the surface Brillouin zone. The results for the relaxed GaAs(110) surface are shown by thick lines. Experimental results, obtained from He-atom scattering and HREELS measurements, are shown as explained in the figure caption.

First of all, it is interesting to note that there are a few 'stomach' gaps in the projected bulk phonon band structure. These arise due to differences in the dispersions of transverse and longitudinal phonons for acoustic and optical vibrations in bulk GaAs along [110]. No propagating bulk states can be found in these gap regions. In general, there is a broad stomach gap, at around 15 meV, along $\overline{\mathrm{X}}-\overline{\mathrm{M}}-\overline{\mathrm{X}}'$ in the surface Brillouin zone. In particular, the gap regions at various symmetry points are as follows: 13.1–18.2 meV, 26.3–28.8 meV, and 28.8–30.3 meV at $\overline{\mathrm{X}}$; 14.1–22.2 meV, 24.4–25.0 meV, and 28.9–30.0 meV at $\overline{\mathrm{M}}$; and 12.0–15.6 meV and 24.5–28.4 meV at $\overline{\mathrm{X}}'$. Any solutions found in these regions will be true surface states.

In figure 2 we have shown the dispersion of phonon modes on the relaxed surface as calculated in this work. We have considered most of the states corresponding to vibrations of atoms in the top three surface layers. In the discussion below we will mainly consider modes with vibrations of atoms in the top two layers, but occasionally with vibrations including the third layer.

Table 1. Calculated surface phonon frequencies for GaAs(110) at the $\overline{\Gamma}$ point and their comparison with experiments and available theoretical calculations. The modes have been classified according to the irreducible representations A′ and A″ of the point group symmetry of the surface unit cell. Only some surface modes are shown, and others can be found in figure 5. The results in parentheses indicate complex displacement patterns with large amplitude at the outermost surface atoms. Frequencies are given in meV.

Reference	A″			A′					
Present results	11.96	28.68	32.18	10.99	(15.77)	20.88	22.80	30.46	35.80
ab initio [26]	(8.6)	31.1	31.7	(11.1)	14.6	(17.7)	23.2		35.8
ab initio [25]		30.0	32.2		16.5		23.7	30.9	34.6
ab initio [24]				11.0	13.3			27.3	34.1
Bond charge [20]				9.6					
Tight binding [22]	9.8								
Tight binding [21]				10.7					
He scattering [10]				10.0					
HREELS [14]					17.5		23.2		35.0
HREELS [17]				10.5	16.5		21.1		35.8

Before proceeding with our discussion we remark that HREELS measurements have typical errors of ± 1 meV and that the *ab initio* results presented by three different groups may differ by up to 2 meV (except for at one particular frequency for which the various results differ by more than 4 meV—see table 1).

3.1. The effect of surface relaxation on vibrations

For the unrelaxed surface we consider the ideally terminated bulk positions for the Ga and As ions, and place bond charges of magnitude $Z/2$ at their bulk positions along each of the dangling bonds from Ga and As atoms. This results in 22 ions and 46 BCs (42 of magnitude Z and 4 of magnitude $Z/2$) within the unrelaxed unit cell. For the relaxed surface geometry we consider the Ga dangling orbital to contain no bond charge and the As dangling orbital to contain a BC of magnitude Z, in accordance with the well established view [4–6].

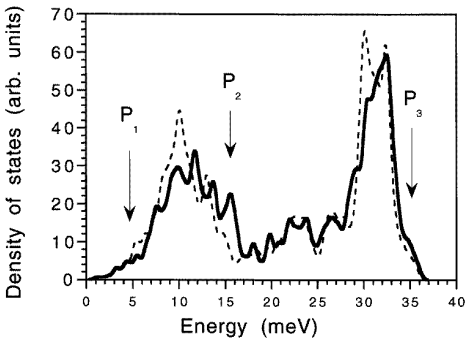

Figure 3. The density of phonon states on GaAs(110). The solid curve was obtained from the (110) slab supercell calculation with the relaxed surface geometry, while the dotted curve shows the density of states with the ideally terminated surface geometry. Some important differences are highlighted by arrows and discussed in the text.

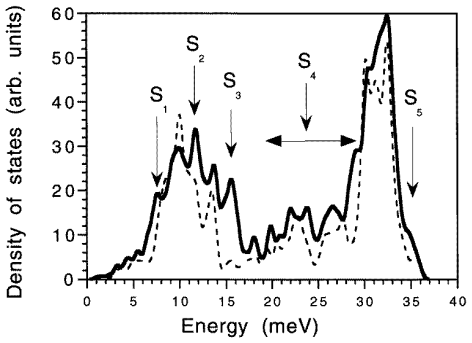

Figure 4. The density of phonon states for the slab supercell with the relaxed surface geometry (solid curve) is compared with the bulk density of states (dotted curve). Important surface features are indicated as peaks S_1 to S_5. The peak S_1 is related to the Rayleigh wave, and the peak S_5 corresponds to the Fuchs–Kliewer phonon branch.

We make a few observations regarding the importance of atomic relaxation on surface phonon modes. Firstly, there are a few relaxation-derived surface states, i.e. such states are not observed with the unrelaxed geometry. Secondly, some of the states identified for the unrelaxed geometry are found to change upwards in energy by up to 3 meV upon relaxation of the surface. However, amplitudes of atomic vibrations do not change by more than 20% when surface relaxation is considered. In figure 2 we have shown, with dashed curves, two specific examples of true surface states in the acoustic range for the unrelaxed geometry along the $\overline{\mathrm{X}}'$–$\overline{\mathrm{M}}$ direction. The lower mode is a Rayleigh mode and is shifted in energy by about 2 meV from the same mode for the relaxed geometry. The upper mode shows a dispersion different to that of its counterpart upon relaxation: whereas at $\overline{\mathrm{X}}'$ there is very little difference between the unrelaxed surface frequency and the relaxed surface frequency, at $\overline{\mathrm{M}}$ the unrelaxed surface frequency lies 2 meV below the relaxed surface frequency. It should be mentioned here that we can expect surface frequencies to alter by up to 1 meV upon consideration of reasonable changes in surface atomic geometry and dangling position.

In figure 3 we have plotted the phonon density of states of the repeated slab geometry with the ideally terminated surface geometry (dashed curve) and with the relaxed surface geometry (solid curve). It is evident that the surface relaxation gives rise to significant changes in the density of states. In particular, we identify important changes in three energy ranges. Firstly, in the lower part of the acoustic range at around 5 meV there is a small peak (P_1) in the density of states for the unrelaxed geometry, which is washed away when the relaxed geometry is considered. Secondly, in the LA–TA gap region there develops a strong peak (P_2) for the relaxed geometry. Furthermore, for the relaxed geometry there is a

small peak (P_3) in the gap between the long-wavelength LO and TO bulk frequencies which is not seen for the unrelaxed geometry.

Table 2. Calculated surface phonon frequencies (in meV) for some modes on GaAs(110) at $\overline{X}'$. The representations A′ and A″ represent the sagittal (SG) and shear horizontal (SH) polarizations, respectively. Our results are compared with available experimental data. RW indicates the Rayleigh mode, and A_1 is the zone-boundary acoustic mode discussed in the experimental literature and referred to in the text.

Reference	A″			A′						
Present results	6.82	28.94	6.40	7.69	10.46	12.96	25.94	27.86	29.76	35.11
ab initio [25]	6.13		5.78	7.58						35.70
He scattering [16]			5.6	7.3						
HREELS [17, 18]			5.7	7.2	10.5					35.8
			RW	RW	A_1					

Table 3. Calculated surface phonon frequencies (in meV) for some modes on GaAs(110) at $\overline{X}$. The sums of the squares of the sagittal (SG) and shear horizontal (SH) components of the modes are given in square brackets. Our results are compared with available theoretical and experimental results. The results shown in parentheses describe complex displacement patterns with large amplitude at the topmost surface atoms. RW indicates the Rayleigh mode, and A_1 and A_2 are the zone-boundary acoustic modes discussed in the experimental literature and referred to in the text.

Reference	Modes at $\overline{X}$								
Present results	8.73	9.51	9.95	13.45	13.86	21.01	28.22	29.28	33.23
$\left[\sum U_{SG}^2\right]$	0.98	0.86	0.70	0.47	0.48	0.90	0.90	0.70	0.40
$\left[\sum U_{SH}^2\right]$	0.02	0.14	0.30	0.53	0.52	0.10	0.10	0.30	0.60
ab initio [26]	8.7	8.9	11.1	13.0	14.2	22.7	28.2	32.0	35.5
$\left[\sum U_{SG}^2\right]$	0.68	0.70	0.51	0.50	0.51	0.93	0.79	0.89	0.42
$\left[\sum U_{SH}^2\right]$	0.32	0.30	0.49	0.50	0.49	0.07	0.21	0.11	0.58
ab initio [25]	8.6	8.9	10.0	13.0	14.5		27.4		34.4
ab initio [24]	4.4	8.8	11.0		13.6	22.3		30.0	33.5
Bond charge [20]	7.6		9.5		13.3				
HREELS [17, 18]	8.6 (RW)		10.5 (A_1)		14.8 (A_2)	21. 5			34.8

3.2. The surface vibrational spectrum

As seen from figure 2, our results for the relaxed surface geometry are in very good overall agreement with experimental measurements except for in a few cases as noted below. A detailed comparison of our results with experimental and recent *ab initio* results at the $\overline{\Gamma}$, $\overline{X}$ and $\overline{X}'$ points is presented in tables 1–3. Also given in tables 1 and 2 are the results from tight-binding studies [21, 22] and the BCM work of Santini *et al* [19, 20].

In particular, our theoretically obtained dispersion of the Rayleigh mode along $\overline{\Gamma}$–$\overline{X}$ and $\overline{\Gamma}$–$\overline{X}'$ at the bottom edge of the projected bulk acoustic range maps out the experimentally

observed result very well. We also find a rather flat band at around 10 meV along both of these azimuths, in agreement with experiment. There is also good agreement between theory and experiment for the state near 13 meV at around the $\overline{\mathrm{X}}$ point in the $\overline{\Gamma}$–$\overline{\mathrm{X}}$ direction. However, we predict a few modes which have not been observed experimentally for the reason explained in the next section.

In the recent HREELS measurements Nienhaus and Mönch [17, 18] have detected a rather flat surface phonon band along both $\overline{\Gamma}$–$\overline{\mathrm{X}}$ and $\overline{\Gamma}$–$\overline{\mathrm{X}}'$, lying in the energy range 34.8–35.8 meV. This is the long-wavelength optical surface or Fuchs–Kliewer phonon with a frequency of 35.8 meV at $\overline{\Gamma}$. Noting that the experimental measurements and theoretical estimates have error margins of 1 meV, this band can be said to nearly coincide with the top of the bulk GaAs phonon frequency spectrum at 35.2 meV. In our work we find, as shown in figure 2 and tables 1–3, that the Fuchs–Kliewer (FK) phonon branch lies in the bulk TO(Γ)–LO(Γ) gap range (33.6–36.4 meV). This is what is expected, as we now show. The frequency of the Fuchs–Kliewer phonon is given by the expression [35]

$$\omega_{FK} = \sqrt{\frac{\epsilon(0)+1}{\epsilon(\infty)+1}}\omega_{TO} \tag{10}$$

where $\epsilon(0)$ and $\epsilon(\infty)$ are the static and high-frequency dielectric constants of the substrate material. The Lyddane–Sachs–Teller relation between the TO(Γ) and LO(Γ) frequencies is

$$\omega_{LO}^2/\omega_{TO}^2 = \epsilon(0)/\epsilon(\infty). \tag{11}$$

As $\epsilon(0) > \epsilon(\infty)$, from the above two equations it is easy to establish that the Fuchs–Kliewer frequency lies between the TO(Γ) and LO(Γ) frequencies, i.e.

$$\omega_{TO} < \omega_{FK} < \omega_{LO}. \tag{12}$$

Therefore, we expect our prediction of the FK phonon frequency, and its dispersion along the various symmetry directions, to be correct.

The density of phonon modes from our slab supercell calculation is shown in figure 4. For comparison we have also shown the phonon density of states for bulk GaAs. Atomic vibrations on the GaAs(110) surface lead to new peaks in the phonon density of states. These are labelled S_1 to S_5 in the figure. There are a few small intensity peaks, indicated by S_4, which lie in the energy range 20–29 meV and are resonant with the bulk density of states. The peak S_1 at around 7 meV is due to the Rayleigh waves, S_2 is a peak due to resonant states in the range of the so-called A_1 mode, S_3 at around 16 meV is due to localized surface states in the stomach gap, and S_5 at around 35 meV is due to the highest-lying true and resonant surface states forming the Fuchs–Kliewer branch.

3.3. Polarization and localization of surface modes

In general, the vibrational modes at the centre of the surface Brillouin zone ($\overline{\Gamma}$), as well as along $\overline{\Gamma}$–$\overline{\mathrm{X}}'$, of the III–V(110) surface can be classified according to the irreducible representations of the point group symmetry C_s (or $\mathrm{C}_{1\mathrm{h}}$ or m) of the surface unit cell. Accordingly [36], atomic vibrations along $[\bar{1}10]$, i.e. along the III–V zigzag chain direction, are represented as A″ modes, and vibrations perpendicular to the chain direction are represented as A′. Such a clear classification is not possible along the symmetry directions $\overline{\Gamma}$–$\overline{\mathrm{X}}$ and $\overline{\Gamma}$–$\overline{\mathrm{M}}$ in the surface Brillouin zone. Along these directions modes show a mixture of shear horizontal and sagittal-plane (defined by the direction of the two-dimensional phonon wavevector and the surface-normal direction) polarizations.

In figure 2 we have plotted the surface phonon spectrum corresponding to atomic vibrations in the top three layers of the slab. As we said earlier, in this section we will

describe the energies and polarizations of the modes for which vibrational amplitudes are largest for the first-layer and second-layer surface atoms. Consideration of atomic vibrations in the top two layers of the slab is equivalent to solving a dynamical problem with four atoms per unit cell. This consideration leads to 12 vibrational modes for a given surface phonon wave vector, with the lowest three being acoustic in nature.

3.3.1. At the $\overline{\Gamma}$*-point.* At the $\overline{\Gamma}$ point we have classified 4 of the 12 modes as A″ modes, and 8 as A′ modes. The displacement patterns of these modes are presented in figure 5.

The lowest surface frequency, which is at 4.55 meV, is an acoustic mode with all the four surface atoms (in the top and second layers) vibrating in the A″ mode. The second acoustic surface frequency at 6.00 meV corresponds to the A′ mode of vibration of the four atoms along $[00\bar{1}]$. The highest acoustic surface frequency at $\overline{\Gamma}$ lies at 9.02 meV and corresponds to an A′ mode of vibration along $[\bar{1}\,\bar{1}0]$.

The lowest surface optical frequency at 10.99 meV is of the A′ mode and corresponds to the top and second layers vibrating against each other. This mode can also be described as a rotational mode of the GaAs chain on the surface, in agreement with the tight-binding calculation by Wang and Duke [21] who place it at 10.7 meV. Also, this mode agrees very well with the recent pseudopotential calculation of Schmidt *et al* [26] who place it at 11.1 meV. The frequency at 11.96 meV is of the A″ mode and represents the optical vibrational pattern between the top and second layers. At 20.88, 21.90 and 24.04 meV we find complex vibrational patterns of the A′ representation involving atoms in the top and second layers. These frequencies agree very well with the HREELS measurements of a surface mode between 21 and 22 meV by Nienhaus and Mönch [17]. The A′ mode at 22.80 is due to opposing motions of cations and anions in both the top and second layers. (Note that the above surface optical modes lie in the bulk acoustic range.) The frequency at 28.68 meV corresponds to A″-type modes involving top-layer Ga and As atoms. As remarked earlier, these frequencies have not yet been observed experimentally. Vibrations at 32.18 meV correspond to the A″ representation involving the second-layer Ga and As atoms (with a small contribution from top-layer atoms). Finally, at 35.80 meV we find a complex mode of the A′ representation. This corresponds to the vibrations of top-layer Ga and As atoms against each other and that of second-layer Ga and As atoms against each other. The Ga atoms in the two layers vibrate fairly much in phase. Similarly the As atoms in the two layers vibrate in phase. This displacement pattern corresponds to stretching of the Ga–As bond, involving atoms in the first and second layers. For this mode there is also a large amplitude of atomic vibrations in the third layer. Other calculations have predicted the corresponding displacement pattern to be of a bond-stretching character between the first-layer Ga and second-layer As atoms [25, 26], which is consistent with our finding. This frequency agrees very well with the Fuchs–Kliewer phonon observed experimentally [17].

In table 1 we have listed some of the above frequencies and compared them (favourably) with experiment and other theoretical calculations. In addition to the 12 modes discussed above, we have calculated a few other modes. The mode at 15.77 meV is found to correspond to a complex displacement pattern with large amplitude at the outermost surface atoms. The mode at 30.46 meV exhibits a significant amplitude of vibrations in the third layer.

3.3.2. Along the $\overline{\Gamma}$–$\overline{\mathrm{X}'}$ *direction.* As mentioned earlier, surface vibrations along $\overline{\Gamma}$–$\overline{\mathrm{X}'}$ can be classified according to the A′ and A″ polarization representations. Some of the frequencies at $\overline{\mathrm{X}'}$ are listed in table 2. In general our results agree well with the recent *ab*

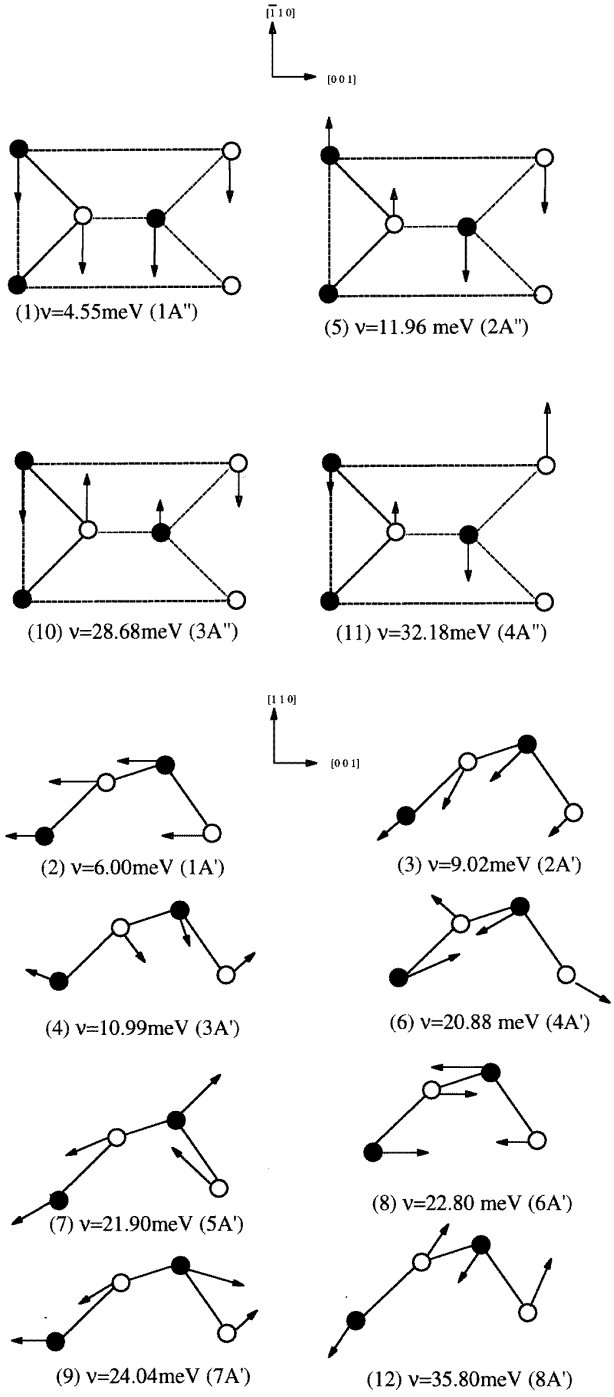

Figure 5. Atomic displacement patterns of surface phonons at the $\bar{\Gamma}$ point. Considering atomic vibrations in the top and subsurface layers, we have 12 modes: four A″ symmetry modes with vibrations along [$\bar{1}$10], the Ga–As zigzag chain direction, and eight A′ symmetry modes with vibrations perpendicular to the chain direction. The lowest acoustic mode is of A″ symmetry, while the other two acoustic modes are of A′ symmetry. The modes are enumerated in ascending order of frequencies.

initio calculations by Fritsch *et al* [25], and experimental data obtained by He-scattering [16] and HREELS [17, 18] techniques. In particular, in the bulk TA range we find four modes. The modes at 6.4 and 7.69 meV have A′ character and can be compared with similar modes at 5.78 and 7.58 meV in the work of Fritsch *et al*. Both of these modes have been measured using He scattering and HREELS (in the range 5.6–7.3 meV). The mode at 6.82 meV compares well with the mode at 6.13 in the work of Fritsch *et al*, but cannot be detected experimentally as it has A″ character. We have also calculated a mode lying at 10.46 meV which has been measured by HREELS at 10.5 meV (and referred to as the A_1 mode in the literature). This mode, however, has not been identified in the theoretical work of Fritsch *et al*. In the TA–LA gap we have identified a mode at 12.96 meV of A′ character and this can be compared (favourably) with the mode at 13.44 meV in the work of Fritsch *et al*. We also agree with Fritsch *et al* in their observation that this mode results from vibrations of the top-layer Ga atoms perpendicular to the zigzag chain direction. Finally, the mode at 35.11 meV also has A′ character and belongs to the Fuchs–Kliewer phonon branch lying above the projected bulk phonon spectrum. This can be compared with the mode at 35.70 meV in the theoretical work of Fritsch *et al* and at 35.8 meV in the HREELS measurement. However, we find that this mode involves displacements of first-, second- and third-layer atoms. The calculated dispersion of the Rayleigh mode along $\overline{\Gamma}$–$\overline{X}'$ agrees well with that measured in the HREELS and He-scattering experiments.

3.3.3. Along the $\overline{\Gamma}$–$\overline{X}$ *direction.* The recent HREELS measurements [17, 18] have reported five surface modes at the $\overline{X}$ point. Modes at 8.6, 10.5, 14.8 and 21.5 meV lie in the bulk acoustic range, and the mode at 34.8 meV lies near the top of the projected bulk spectrum. The first three of these modes have been labelled in the literature as RW (Rayleigh wave), A_1 and A_2, respectively, and can be compared with the modes at 8.73, 9.95 and 13.86 meV in our work. The experimental mode at 21.5 meV can be compared with the mode at 21.01 meV in our work. Finally, the experimentally observed Fuchs–Kliewer branch mode at 34.8 meV can be compared with our calculation of the mode at 33.23 meV.

As can be seen from table 3, our surface frequencies at $\overline{X}$ agree well with those given in the *ab initio* works of Schmidt *et al* [26] and Fritsch *et al* [25]. However, there is some difference between various theoretical results for the RW wave. Firstly, the *ab initio* work by Di Felice *et al* [24] places it at 4.4 meV which is too low compared with our and other theoretical work. Secondly, while Fritsch *et al* find that this mode is due to in-phase vibrations of the top-layer As and second-layer Ga atoms, we find that this is due to in-phase vibrations of top-layer Ga and second-layer As atoms along the surface normal. The work of Schmidt, on the other hand, predicts this mode to possess 68% of its character as sagittal (SG) polarization, while we predict it to be almost totally polarized as SG. There is good agreement among all theoretical studies and the HREELS measurement for the energy location and polarization behaviour of the A_1 mode. The mode at 13.45 meV agrees well with the theoretical work of Schmidt *et al* and of Fritsch *et al* with respect to its energy location and polarization behaviour: it corresponds to the displacements the top-layer Ga atoms along the zigzag chain direction and the top-layer As atoms perpendicular to the chain direction. Next we predict the A_2 mode to lie at 13.86 meV, in good agreement with other theoretical calculations and the HREELS measurements. As shown here and by Schmidt *et al*, this mode has almost equal amplitudes of SG and SH polarization components. There is also good agreement between our results and that due to Schmidt *et al* for three modes between 20 and 30 meV. Finally, in agreement with the work of Fritsch *et al*, we find that the highest surface phonon mode at $\overline{X}$ has a displacement pattern which is dominated by an

opposing motion of the top-layer Ga atoms and the second-layer As atoms perpendicular to the chain direction. Our work suggests that for this mode there is also a large contribution from the Ga and As atoms in the third layer. This is similar to the displacement pattern of the Fuchs–Kliewer phonon at $\overline{\Gamma}$. The calculated SG and SH components of the polarization amplitude for this mode at $\overline{\mathrm{X}}$ are in the same proportion as found by Schmidt *et al*. The calculated dispersion of the Rayleigh mode along $\overline{\Gamma}$–$\overline{\mathrm{X}}$ agrees well with that measured in the HREELS and He-scattering experiments.

3.3.4. Along the $\overline{\Gamma}$–$\overline{\mathrm{M}}$ *direction.* The calculated dispersion of the Rayleigh mode along $\overline{\Gamma}$–$\overline{\mathrm{M}}$ agrees well with the He-scattering measurements. Also, near the $\overline{\mathrm{M}}$ point the frequencies 7.8 and 14.5 meV obtained from He-scattering experiments are reproduced by our theoretical calculations.

4. Conclusions

In this paper we have calculated the phonon dispersion curves for the GaAs(110) surface by employing the phenomenological bond charge model. We have shown that the results from this method agree well with existing *ab initio* theoretical calculations and experiments. We have provided a more detailed account of surface vibrations than is currently available from experiments or other theoretical calculations, including the work of Santini *et al* who also used the bond charge model. We have found that vibrational frequencies corresponding to the relaxed surface geometry are quite different from those on the ideally terminated surface. In particular, we have noted that a few surface modes are very sensitive to surface relaxation. We have identified energy location and polarization characteristics of various phonon modes at $\overline{\Gamma}$, $\overline{\mathrm{X}}$, $\overline{\mathrm{X}'}$ and $\overline{\mathrm{M}}$, and along the symmetry directions $\overline{\Gamma}$–$\overline{\mathrm{X}}$, $\overline{\Gamma}$–$\overline{\mathrm{X}'}$ and $\overline{\Gamma}$–$\overline{\mathrm{M}}$. Our results agree well with recent HREELS and He-inelastic-scattering measurements for the dispersion of the Rayleigh mode along these symmetry directions, and also for the modes A_1 and A_2 at the zone boundaries ($\overline{\mathrm{X}}$ and $\overline{\mathrm{X}'}$). The agreement between theory and experiment for the dispersion of the Fuchs–Kliewer branch at the top of the bulk spectrum is not as good as is found for the Rayleigh mode, but is acceptable within the error margins inherent to the experimental and theoretical studies. Our studies therefore commend the adiabatic bond charge model as a reliable theoretical technique for the description of the surface dynamics of GaAs(110).

Acknowledgments

One of us (HMT) is grateful to the University of Sakarya, Turkey, for the award of a studentship. The computational work was supported by the EPSRC (UK) through the CSI scheme.

References

[1] Ford W K, Guo T, Lessor D L and Duke C B 1990 *Phys. Rev.* B **42** 8952
[2] Smit L, Derry T E and van der Veen J F 1985 *Surf. Sci.* **150** 245
[3] Huijer A, van Laar J and van Rooy T L 1978 *Phys. Lett.* **65A** 337
[4] Ferraz A C and Srivastava G P 1987 *Surf. Sci.* **182** 161
[5] Alves A, Hebenstreit J and Scheffler M 1990 *Phys. Rev.* B **44** 6188
[6] Umerski A and Srivastava G P 1995 *Phys. Rev.* B **51** 2334
[7] Zhu X, Zhang S B, Louie S G and Cohen M L 1989 *Phys. Rev. Lett.* **63** 2112

[8] Jenkins S J, Srivastava G P and Inkson J C 1995 *Proc. 22nd Int. Conf. on The Physics of Semiconductors* ed D J Lockwood (Singapore: World Scientific) p 435
[9] Carstenssen H, Claessen R, Manzke R and Skibowski M 1990 *Phys. Rev.* B **41** 9880
[10] Harten U and Toennies J P 1987 *Europhys. Lett.* **4** 833
[11] del Pennino U, Betti M G, Mariani C and Abbati I 1989 *Surf. Sci.* **211/212** 557
[12] Matz R and Lüth 1981 *Phys. Rev. Lett.* **46** 500
[13] Dubois L H and Schwarz G P 1982 *Phys. Rev.* B **26** 794
[14] Betti M G, del Pennino U and Mariani C 1989 *Phys. Rev.* B **39** 5887
[15] Chen Y, Nannarone S, Schafer J, Hermanson J C and Lapeyre G J 1989 *Phys. Rev.* B **39** 7653
[16] Doak R B and Nguyen D B 1987 *J. Electron Spectrosc. Relat. Phenom.* **44** 205
[17] Nienhaus H and Mönch W 1995 *Phys. Rev.* B **50** 11 750
[18] Nienhaus H 1994 *PhD Thesis* University of Duisburg, Germany
[19] Santini P, Miglio L, Benedek G and Ruggerone P 1991 *Surf. Sci.* **241** 346
[20] Santini P, Miglio L, Benedek G, Harten U, Ruggerone and Toennies J P 1990 *Phys. Rev.* B **42** 11 942
[21] Wang Y R and Duke C B 1988 *Surf. Sci.* **205** L755
[22] Klein W and Zijing L 1990 *Phys. Rev.* B **41** 5312
[23] Godin T J, LaFemina J P and Duke C B 1991 *J. Vac. Sci. Technol.* B **9** 2282
[24] Di Felice R, Shkrebtii A I, Finocchi F, Bertoni C M and Onida G 1993 *J. Electron Spectrosc. Relat. Phenom.* **64/65** 697
[25] Fritsch J, Pavone P and Schröder U 1993 *Phys. Rev.* Lett **71** 4194
[26] Schmidt W G, Bechstedt F and Srivastava G P 1995 *Phys. Rev.* B **52** 2001
[27] Weber W 1974 *Phys. Rev. Lett.* **33** 371
[28] Weber W 1977 *Phys. Rev.* B **15** 4789
[29] Rustagi K C and Weber W 1979 *Solid State Commun.* **18** 673
[30] Srivastava G P and Kunc K 1988 *J. Phys. C: Solid State Phys.* **21** 5087
[31] Miglio L, Santini P, Ruggerone P and Benedek G 1989 *Phys. Rev. Lett.* **62** 3070
[32] Sanguinetti S, Benedek G, Righetti G and Onida G 1994 *Phys. Rev.* B **50** 6743
[33] Maradudin A A, Montroll E W, Weiss G H, and Ipatova I P 1971 *Theory of Lattice Dynamics in the Harmonic Approximation* 2nd edn (New York: Academic)
[34] Keating P N 1966 *Phys. Rev.* **145** 637
[35] Zangwill A 1992 *Physics at Surfaces* (Cambridge: Cambridge University Press)
[36] Boardman A D, O'Connor D E and Young P A 1973 *Symmetry and its Applications in Science* (Maidenhead: McGraw-Hill)